

Simulation of dynamical (u, d, s, c) domain-wall/overlap quarks at the physical point

Ting-Wai Chiu^{*†} (TWQCD Collaboration)

Institute of Physics, Academia Sinica, Taipei, Taiwan 11529, R.O.C.

Physics Department, National Taiwan Normal University, Taipei, Taiwan 11677, R.O.C.

Physics Department, National Taiwan University, Taipei, Taiwan 10617, R.O.C.

E-mail: twchiu@phys.ntu.edu.tw

We perform hybrid Monte-Carlo simulation of $N_f = 2 + 1 + 1$ lattice QCD with domain-wall quarks at the physical point. The simulation is carried out on the $L^3 \times T = 64^3 \times 64$ lattice with lattice spacing $a \sim 0.064$ fm ($L > 4$ fm, and $M_\pi L > 3$), using the Nvidia DGX-1 (8 V100 GPUs interconnected by the NVLink). To attain the maximal chiral symmetry for a finite extent ($N_s = 16$) in the fifth dimension, we use the optimal domain-wall fermion for the quark action, together with the exact one-flavor action for domain-wall fermion. We outline the salient features of our simulation (without topology freezing, and small residual mass), together with the preliminary result of the masses of π^\pm , K^\pm , and D^\pm .

The 36th Annual International Symposium on Lattice Field Theory - LATTICE2018

22-28 July, 2018

Michigan State University, East Lansing, Michigan, USA.

^{*}Speaker.

[†]This work is supported by the Ministry of Science and Technology (Nos. 107-2119-M-003-008, 105-2112-M-002-016, 102-2112-M-002-019-MY3), and National Center for Theoretical Sciences (Physics Division).

1. Introduction

The holy grail of lattice QCD is to simulate QCD with all quarks at their physical masses, with sufficiently large volume and fine lattice spacing, then to extract physics from these gauge ensembles. Since the t quark is extremely short-lived and it decays to W -boson and $b/s/d$ quarks before it can interact with other quarks through the gluons, it can be neglected in QCD simulations. Even after neglecting the t quark, to simulate (u, d, s, c, b) quarks at their physical masses (ranging from $\sim 3 - 4500$ MeV) is still a very challenging problem. For example, if one designs the simulation on a L^4 lattice with $M_\pi L > 4$ and lattice spacing $a < 0.035$ fm such that the b quark mass satisfies $m_b a < 0.8$, then it would require $L/a > 180$, which is beyond the capability of the current generation of supercomputers with $\sim 100 - 200$ Petaflops/s.

Now if we neglect the b quark, then lattice QCD with physical (u, d, s, c) quarks can be simulated on a 64^4 lattice with lattice spacing $a \sim 0.067$ fm, which satisfies $m_c a < 0.6$, $M_\pi L > 3$, and $L > 4$ fm, as shown in Fig. 1. The hybrid Monte-Carlo (HMC) [1] simulation of this $N_f = 2 + 1 + 1$ lattice QCD can be performed with the current generation of supercomputers, however, the degree of difficulties depends on which kind of lattice fermion is used.

It took 24 years (1974-1998) to realize that lattice QCD with exact chiral symmetry [2, 3] is the ideal theoretical framework to study the non-perturbative physics from the first principles of QCD. However, it is challenging to perform the Monte Carlo simulation such that the chiral symmetry is preserved to a very high precision and all topological sectors are sampled ergodically. Moreover, the computational requirement for lattice QCD with domain-wall quarks on a 5-dimensional lattice is 10-100 times more than their counterparts with traditional lattice fermions (e.g., Wilson, staggered, and their variants).

In this talk, I report the first HMC simulation of lattice QCD with physical $N_f = 2 + 1 + 1$ domain-wall quarks. The simulation is performed on a 64^4 lattice with the extent $N_s = 16$ in the fifth dimension, using just one GPU server on the table top, the Nvidia DGX-1 (with eight V100 GPUs interconnected by the NVLink, and total device memory $16 \times 8 = 128$ GB). In general, to simulate $N_f = 2 + 1 + 1$ lattice QCD a 64^4 lattice with any lattice Dirac operator D usually requires memory much larger than 128 GB, since each one-flavor pseudofermion action is expressed as the rational approximation of $\Phi^\dagger (D^\dagger D)^{-1/2} \Phi$, requiring a large number (proportional to the number of poles in the rational approximation) of long vectors in computing the fermion forces in the molecular dynamics. However, for domain-wall fermion, one can use the exact one-flavor pseudofermion action (EOFA) with a positive-definite and Hermitian Dirac operator [4]. Moreover, using EOFA for $N_f = 2 + 1 + 1$ lattice QCD with domain-wall quarks not only saves the memory such that the HMC simulation on a $64^4 \times 16$ lattice can be fitted into 128 GB device memory of Nvidia DGX-1, but also enhances the HMC efficiency significantly.

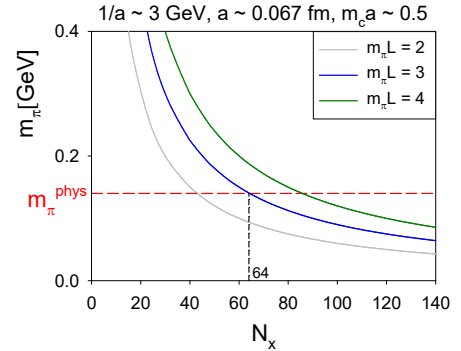


Figure 1: Design lattice QCD with physical (u, d, s, c) quarks.

2. Generation of the gauge configurations

As pointed out in Ref. [5], for domain-wall fermions, to simulate $N_f = 2 + 1 + 1$ amounts to simulate $N_f = 2 + 2 + 1$, according to the identity

$$\frac{\det \mathcal{D}(m_{u/d})}{\det \mathcal{D}(m_{PV})} \frac{\det \mathcal{D}(m_{u/d})}{\det \mathcal{D}(m_{PV})} \frac{\det \mathcal{D}(m_s)}{\det \mathcal{D}(m_{PV})} \frac{\det \mathcal{D}(m_c)}{\det \mathcal{D}(m_{PV})} \quad (2.1)$$

$$= \left(\frac{\det \mathcal{D}(m_{u/d})}{\det \mathcal{D}(m_{PV})} \right)^2 \left(\frac{\det \mathcal{D}(m_c)}{\det \mathcal{D}(m_{PV})} \right)^2 \frac{\det \mathcal{D}(m_s)}{\det \mathcal{D}(m_c)}, \quad (2.2)$$

where $\mathcal{D}(m_q)$ denotes the domain-wall fermion operator with bare quark mass m_q , and m_{PV} the mass of the Pauli-Villars field. Since the simulation of 2-flavors is faster than the simulation of one-flavor, it is better to simulate $N_f = 2 + 2 + 1$ than $N_f = 2 + 1 + 1$. In this study, we use (2.2) for our HMC simulations.

For the gluon fields, we use the Wilson plaquette gauge action at $\beta = 6/g_0^2 = 6.20$. For the quark fields, we use the optimal domain-wall fermion [6], where the optimal weights $\{\omega_s, s = 1, \dots, N_s\}$ has the R_5 symmetry [7]. Then the effective 4-dimensional lattice Dirac operator is exactly equal to the "shifted" Zolotarev optimal rational approximation of the overlap operator, with the approximate sign function $S(H)$ satisfying the bound $0 \leq 1 - S(\lambda) \leq 2d_Z$ for $\lambda^2 \in [\lambda_{min}^2, \lambda_{max}^2]$, where d_Z is the maximum deviation $|1 - \sqrt{x}R_Z(x)|_{\max}$ of the Zolotarev optimal rational polynomial $R_Z(x)$ of $1/\sqrt{x}$ for $x \in [1, \lambda_{max}^2/\lambda_{min}^2]$, with degrees $(n-1, n)$ for $N_s = 2n$.

For the two-flavor parts, we use the pseudofermion action for 2-flavors of optimal domain-wall quarks, as defined in Eq. (14) of Ref. [8]. For the one-flavor part, we use the exact pseudofermion action for one-flavor domain-wall fermion, as defined by Eq. (23) of Ref. [4]. The parameters of the pseudofermion actions are fixed as follows. For the $\mathcal{D}(m_q)$ defined in Eq. (2) of Ref. [8], we fix $c = 1, d = 0, m_0 = 1.3, N_s = 16$, and $\lambda_{max}/\lambda_{min} = 6.20/0.05$. Thus $H = H_w$ and $m_{PV} = 2.6$.

We perform the HMC simulation of (2+1+1)-flavors QCD on the $L^3 \times T = 64^3 \times 64$ lattice, with the quark masses $m_{u/d}a = 0.00125, m_s a = 0.04$, and $m_c a = 0.55$, which are fixed by the masses of the charged pion $\pi^\pm(140)$, and the vector mesons $\phi(1020)$ and $J/\psi(3097)$ respectively. The algorithm for simulating 2-flavors of optimal domain-wall quarks has been outlined in Ref. [8], while the exact one-flavor algorithm (EOFA) for domain-wall fermions has been presented in Ref. [4]. In the molecular dynamics, we use the Omelyan integrator [9], and the Sexton-Weingarten multiple-time scale method [10]. Moreover, we introduce auxiliary heavy fermion fields with masses m_H ($m_q \ll m_H \ll m_{PV}$) similar to the case of the Wilson fermion [11], the so-called mass preconditioning. For the 2-flavors parts, mass preconditioning is only applied to the $\mathbf{u/d}$ quark factor of (2.2) with two levels of heavy masses $m_{H_1}a = 0.01$ and $m_{H_2}a = 0.1$. For the one-flavor part, a novel mass preconditioning has been devised for the EOFA [12] which is $\sim 20\%$ faster than the mass preconditioning we have used in Ref. [4]. Also, based on the fact that in EOFA the fermion force of the ϕ_1 field is much smaller than that of the ϕ_2 field, the gauge momentum updating by these two forces can be set at two different time scales.

The simulation is performed with one GPU server, Nvidia DGX-1, with eight V100 GPUs interconnected by the NVLink, and total device memory 128 GB. The schematic diagram of DGX-1 is shown in Fig. 2. Each NVLink provides a point-to-point connections with data rate of 25 Gbit/s per data lane per direction, and the total data rate for the Nvidia DGX-1 is 300 GByte/s

for the total system, sum of input and output data streams. The NVLink plays the crucial role in reducing the bottleneck in data communication between GPUs such that the performance of the entire system can attain almost the perfect scaling with the number of GPUs. For conjugate gradient with 8 GPUs under OpenMP, we export OpenMP environment to re-map the 8 GPUs in a circle such that each GPU can access its neighbors P2P (peer-to-peer) through NVLinks, and also each CPU handles 4 GPUs. Our HMC simulation code attains 10 Tflops/s (sustained) on Nvidia DGX-1, and each HMC trajectory takes about one day. We have generated about 50 HMC trajectories after thermalization. Then sampling one configuration every 5 trajectories, we have 10 configurations for the preliminary measurement of physical observables.

To determine the lattice scale, we use the Wilson flow [13, 14] with the condition

$$\{t^2 \langle E(t) \rangle\}_{t=t_0} = 0.3,$$

and obtain $\sqrt{t_0}/a = 2.2285(18)$ for 50 HMC trajectories. Using $\sqrt{t_0} = 0.1416(8)$ fm obtained by the MILC Collaboration for the $(2+1+1)$ -flavors QCD [15], we have $a^{-1} = 3.104 \pm 0.018$ GeV.

3. Characteristics of the simulation

First, we investigate the effects of chiral symmetry breaking due to finite $N_s = 16$, by computing the residual mass of each quark flavor, according to the formula derived in Ref. [16]. The residual masses of **u/d**, **s**, and **c** quarks are listed in Table 1. We see that the residual mass of the **u/d** quark is $\sim 3\%$ of its bare mass, amounting to

0.11(1) MeV, which is expected to be smaller than other systematic uncertainties. The residual masses of **s** and **c** quarks are even smaller, 0.03(4) MeV, and 0.01(4) MeV respectively. This demonstrates that the optimal DWF can preserve the chiral symmetry to a high precision, for both light and heavy quarks.

Next, we examine the evolution of the topological charge (Q_{top}) in our HMC simulation. Using the Atiyah-Singer index theorem, the topological charge can be measured by the index of the massless overlap-Dirac operator. However, to project the zero modes of the massless overlap-Dirac operator for the 64^4 lattice is prohibitively expensive. On the other hand, the clover topological

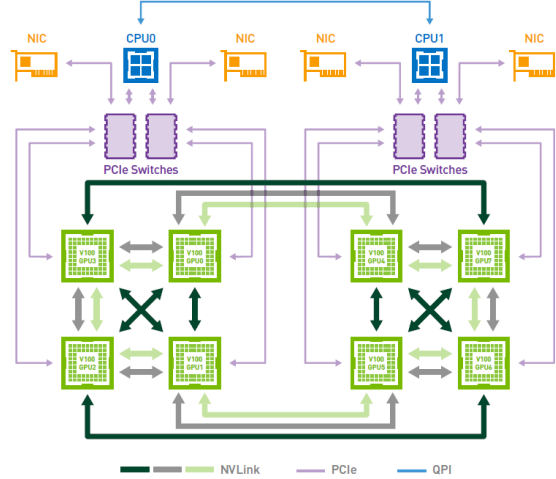


Figure 2: Schematic diagram of DGX-1 from the White Paper “NVIDIA DGX-1 With Tesla V100 System Architecture” (Nvidia Corporation).

Table 1: The residual masses of **u/d**, **s**, and **c** quarks.

quark	$m_q a$	$m_{res} a$	m_{res} [MeV]
u/d	0.00125	$3.61(22) \times 10^{-5}$	0.11(1)
s	0.040	$1.09(14) \times 10^{-5}$	0.03(4)
c	0.550	$0.42(14) \times 10^{-5}$	0.01(4)

charge $Q_{\text{clover}} = \sum_x \varepsilon_{\mu\nu\lambda\sigma} \text{tr}[F_{\mu\nu}(x)F_{\lambda\sigma}(x)] / (32\pi^2)$ is not reliable [where the matrix-valued field tensor $F_{\mu\nu}(x)$ is obtained from the four plaquettes surrounding x on the $(\hat{\mu}, \hat{\nu})$ plane], unless the gauge configuration is sufficiently smooth. The smoothness can be attained by the Wilson flow which is a continuous-smearing process to average gauge field over a spherical region of root-mean-square radius $R_{\text{rms}} = \sqrt{8t}$, where t is the flow time. Theoretically, if a gauge configuration has been flowed for a sufficiently long time to satisfy the condition [14, 17, 18]

$$\min_{\text{plaq}} \left\{ \frac{1}{3} \text{Re tr } U_{\text{plaq}} \right\} > \frac{44}{45} \simeq 0.978, \quad (3.1)$$

then Q_{clover} would be close to an integer, and further Wilson flow acting on this configuration would not change the integer part of Q_{clover} . In other words, applying the Wilson flow to an ensemble of lattice gauge configurations for a sufficiently long time can let them fall into topological sectors, similar to the gauge fields in the continuum theory. In practice, some configuration may take a very long flow time (e.g., $t > 128$) in order to satisfy the condition (3.1), especially for a large lattice like 64^4 . We observe that if the flow equation is integrated from $t = 0$ to $t = 64$ with $\Delta t = 0.01$, then the condition (3.1) is satisfied

by all HMC trajectories generated so far, and the integer value of Q_{clover} becomes a constant for a long interval of flow time before $t = 64$, thus $Q_{\text{top}} = [Q_{\text{clover}}]$ is well-defined. In Fig. 3, the evolution of $Q_{\text{clover}}(t = 64)$ of 31 successive HMC trajectories is plotted. Evidently, the HMC simulation does not suffer from topology freezing, and will likely sample all topological sectors ergodically when the number of trajectories becomes sufficiently large.

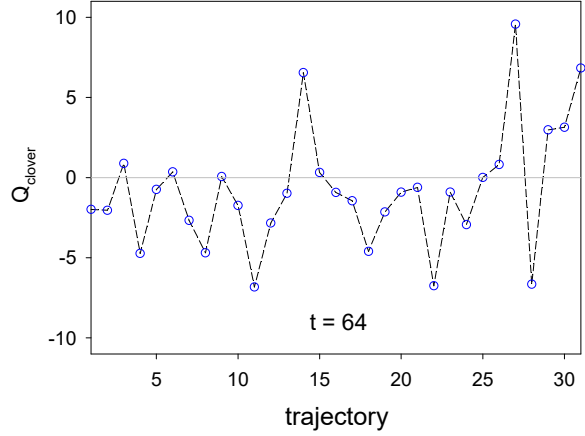


Figure 3: The evolution of the topological charge of 31 successive HMC trajectories.

4. Preliminary result of the masses of π^\pm , K^\pm and D^\pm

With 50 thermalized HMC trajectories, we sample one configuration every 5 trajectories, then we have 10 configurations for the measurement of physical observables. In Fig. 4, the time-correlation functions of $\bar{u}\gamma_5\mathbf{d}$, $\bar{u}\gamma_5\mathbf{s}$, and $\bar{d}\gamma_5\mathbf{c}$ are plotted in the left-panel, while their effective masses are plotted on the right-panel. The fitting results are summarized in Table 2. Our preliminary result of the masses of π^\pm , K^\pm , and D^\pm are in good agreement with the PDG values, suggesting that the quark masses in our HMC simulation are close to the physical ones, though in the limit of isospin symmetry.

5. Conclusion and Outlook

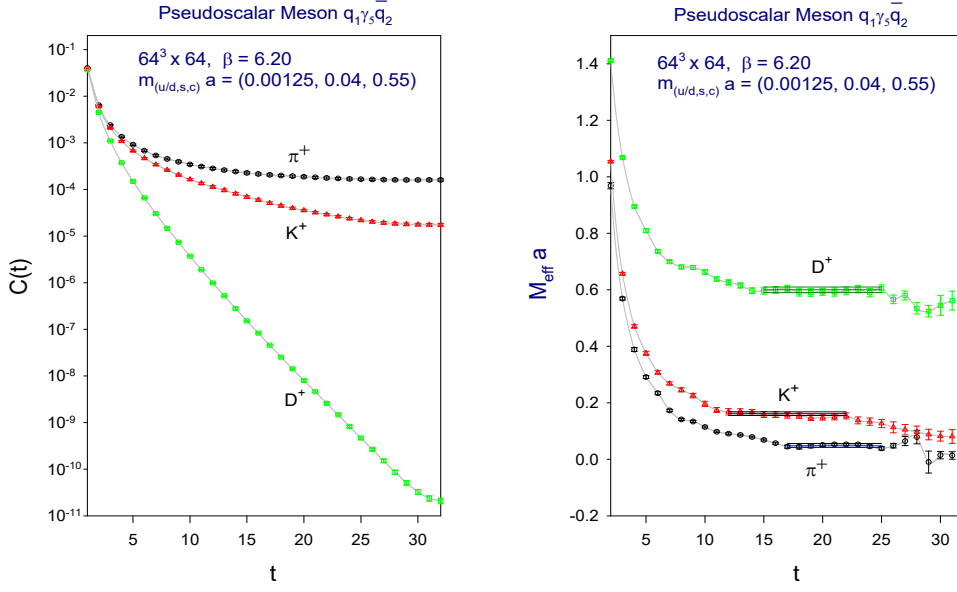


Figure 4: The time-correlation function (left panel) and the effective mass (right panel) of π^\pm , K^\pm , and D^\pm .

This study asserts that it is feasible to simulate lattice QCD with ($\mathbf{u}, \mathbf{d}, \mathbf{s}, \mathbf{c}$) optimal domain-wall quarks at their physical masses, with good chiral symmetry, and without topology freezing. The exact pseudofermion action for one-flavor DWF plays the crucial role in the simulation, not only to save the memory consumption such that the entire HMC simulation on the $64^3 \times 64 \times 16$ lattice can be fitted into the 128 GB device memory of Nvidia DGX-1, but also to enhance the HMC efficiency significantly.

To generate gauge ensembles with physical ($\mathbf{u}, \mathbf{d}, \mathbf{s}, \mathbf{c}$) domain-wall quarks, we will be in a good position to determine physical quantities, e.g., the hadron mass spectra, the decay constants, and the weak matrix elements, as well as to address some subtle nonperturbative physics, e.g., the GIM mechanism, and the $\Delta I = 1/2$ rule. Besides lattice QCD at zero temperature, we are also simulating lattice QCD at finite temperature with $N_f = 2 + 1 + 1$ physical domain-wall quarks, for $T = 130 - 500$ MeV, which is essential for understanding the role of QCD in the early universe.

In retrospect, at the beginning of TWQCD domain-wall project in 2008, we started with the simulation of 2-flavors QCD on the $16^3 \times 32 \times 16$ lattice ($a \sim 0.1$ fm) with pion mass ~ 200 MeV [19]. The simulation can be fitted into one Nvidia GTX-280 card with 1 GB device memory, attaining ~ 150 Gflops/s (sustained). It was hard to imagine that after 10 years, with the advancement in both machine and algorithm, now it is feasible to simulate $N_f = 2 + 1 + 1$ lattice QCD with physical domain-wall quarks, and the entire simulation can be fitted into one GPU server on the table top,

Table 2: The preliminary result of the masses of the lowest-lying pseudoscalar meson states obtained in this work, in comparison with the PDG values.

$\bar{q}_1 \gamma_5 q_2$	$[t_1, t_2]$	χ^2/dof	Mass[MeV]	PDG
$\bar{u} \gamma_5 d$	[17,24]	0.65	141(8)	π^\pm (140)
$\bar{u} \gamma_5 s$	[12,22]	0.81	495(7)	K^\pm (494)
$\bar{d} \gamma_5 c$	[15,22]	0.63	1874(18)	D^\pm (1870)

at the speed about one trajectory per day. To look forward, the simulation of $N_f = 1 + 1 + 1 + 1$ QCD with physical domain-wall quarks is already around the corner, while that with ($\mathbf{u}, \mathbf{d}, \mathbf{s}, \mathbf{c}, \mathbf{b}$) physical domain-wall quarks will be feasible in early 2020s, most likely requiring more than just one table-top GPU server.

Acknowledgement

The author is grateful to Jensen Huang of Nvidia Corporation, for his help to realize this study. Also, the author appreciates the technical support from Nvidia Taipei office. This work is supported by the Ministry of Science and Technology (Grant Nos. 107-2119-M-003-008, 105-2112-M-002-016, 102-2112-M-002-019-MY3), and National Center for Theoretical Sciences (Physics Division). The author also thanks the members of TWQCD collaboration, in particular, Yu-Chih Chen, Han-Yi Chou, Tung-Han Hsieh, and Yao-Yuan Mao, for their contributions in the TWQCD code development.

References

- [1] S. Duane, A. D. Kennedy, B. J. Pendleton and D. Roweth, Phys. Lett. B **195**, 216 (1987).
- [2] D. B. Kaplan, Phys. Lett. B **288**, 342 (1992) [arXiv:hep-lat/9206013].
- [3] H. Neuberger, Phys. Lett. B **417**, 141 (1998) [hep-lat/9707022].
- [4] Y. C. Chen, T. W. Chiu [TWQCD Collaboration], Phys. Lett. B **738**, 55 (2014) [arXiv:1403.1683 [hep-lat]].
- [5] Y. C. Chen, T. W. Chiu [TWQCD Collaboration], Phys. Lett. B **767**, 193 (2017) [arXiv:1701.02581 [hep-lat]].
- [6] T. W. Chiu, Phys. Rev. Lett. **90**, 071601 (2003) [hep-lat/0209153].
- [7] T. W. Chiu, Phys. Lett. B **744**, 95 (2015) [arXiv:1503.01750 [hep-lat]].
- [8] T. W. Chiu [TWQCD Collaboration], J. Phys. Conf. Ser. **454**, 012044 (2013) [arXiv:1302.6918 [hep-lat]].
- [9] I.P. Omelyan, I.M. Mryglod, and R. Folk, Phys. Rev. Lett. **86**, 898 (2001).
- [10] J. C. Sexton and D. H. Weingarten, Nucl. Phys. B **380**, 665 (1992).
- [11] M. Hasenbusch, Phys. Lett. B **519**, 177 (2001) [hep-lat/0107019].
- [12] Y. C. Chen and T. W. Chiu, arXiv:1710.09621 [hep-lat].
- [13] R. Narayanan and H. Neuberger, JHEP **0603**, 064 (2006) [hep-th/0601210].
- [14] M. Luscher, JHEP **1008**, 071 (2010) Erratum: [JHEP **1403**, 092 (2014)] [arXiv:1006.4518 [hep-lat]].
- [15] A. Bazavov *et al.* [MILC Collaboration], Phys. Rev. D **93**, no. 9, 094510 (2016) [arXiv:1503.02769 [hep-lat]].
- [16] Y. C. Chen, T. W. Chiu [TWQCD Collaboration], Phys. Rev. D **86**, 094508 (2012) [arXiv:1205.6151 [hep-lat]].
- [17] M. Luscher, Commun. Math. Phys. **85**, 39 (1982).
- [18] A. Phillips and D. Stone, Commun. Math. Phys. **103**, 599 (1986).
- [19] T. W. Chiu *et al.* [TWQCD Collaboration], PoS LAT **2009**, 034 (2009) [arXiv:0911.5029 [hep-lat]].